The HKU Scholars Hub   The University of Hong Kong   香港大學學術庫

Title	**Source localization using a sparse representation framework to achieve superresolution**
Author(s)	**Guo, X; Wan, Q; Chang, C; Lam, EY**
Citation	**Multidimensional Systems And Signal Processing, 2010, v. 21 n. 4, p. 391-402**
Issued Date	**2010**
URL	**http://hdl.handle.net/10722/123832**
Rights	**Creative Commons: Attribution 3.0 Hong Kong License**

COMMUNICATION BRIEF

Source localization using a sparse representation framework to achieve superresolution

**Xiansheng Guo · Qun Wan · Chunqi Chang ·
Edmund Y. Lam**

Abstract   We present a source localization approach using resampling within a sparse
representation framework. In particular, the amplitude and phase information of the sparse
solution is considered holistically to estimate the direction-of-arrival (DOA), where a resam-
pling technique is developed to determine which information will give a more precise esti-
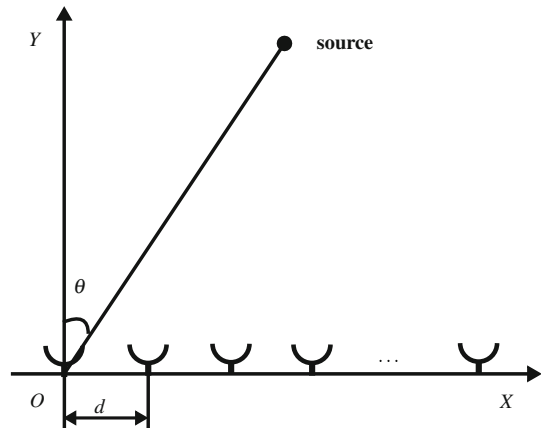mation. The simulation results confirm the efficacy of our proposed method.

1 Introduction

Sparse representation, or sparse coding, of signals has received a lot of attention in recent
years (e.g., Cotter et al. 2002; Gorodnitsky and Rao 1997). One important application of
this signal model is in source localization. Compared with the classical schemes, such as
Multiple Signal Classification (MUSIC) (Schmidt 1986) and estimation of signal parameters
via a rotational invariance technique (ESPRIT) (Roy et al. 1986), the source localization
method using a sparse representation can lead to superresolution in determining the location
of signal sources. This is achieved without the need for a good initialization, without a large
number of snapshots, and with lower sensitivity both to the signal-to-noise ratio (SNR) and
to the correlation of the sources (Maria and Fuchs 2006). Such superresolution of source

X. Guo (✉) · C. Chang · E. Y. Lam
Department of Electrical and Electronic Engineering, University of Hong Kong,
Pokfulam Road, Pokfulam, Hong Kong
e-mail: xsguo@eee.hku.hk

E. Y. Lam
e-mail: elam@eee.hku.hk

X. Guo · Q. Wan
Department of Electronic Engineering, University of Electronic Science and Technology of China,
610054 Chengdu, Sichuan, People's Republic of China

Fig. 1 An example of the signal model

location information is useful for array signal processing and sensor networks (Chow et al. 2007, 2009), which in turn have a wide range of applications ranging from wireless communications, radar, seismic signal processing, to body sensor network and medical imaging.

Sparse source localization methods can be divided into two classes: those with a single measurement vector (SMV) and those with multiple measurement vectors (MMV). The former often uses the indices of nonzero entries in the sparse solution to provide the direction-of-arrival (DOA) estimation. For the latter, the indices of nonzero rows in the sparse solution are used for the DOA estimation instead (Chen and Huo 2006). For simplicity, we refer to both cases as an amplitude-based technique in this paper.

It has been suggested that the performance of existing amplitude-based sparse source localization techniques is mostly affected by the grid distance between adjacent grids of an overcomplete dictionary (Malioutov et al. 2005; Fuchs 1998, 2001). Furthermore, while a refined grid strategy is often efficient to boost the DOA estimation performance (Malioutov et al. 2005), it will in fact be worse when too many grids are generated in the dictionary due to the coherence of its entries. Additionally, too many atoms in an overcomplete dictionary will incur a heavy computational burden, which is unsuitable for practical implementations.

In this paper, we propose an alternative: a phase-based technique that can be synergistically combined with the existing amplitude-based method. A resampling method is used to determine which is best for the DOA estimation. Thus, in addition to the merits of sparse source localization mentioned above, our method can also avoid the need for too many grids in the dictionary.

2 Problem formulation

2.1 The signal model

We consider a uniform linear array (ULA) of M omnidirectional sensors receiving K stationary random signals from far-field point sources. This is depicted in Fig. 1, where the first sensor on the left is the reference point. Throughout this paper, we assume that the signal number is known a priori (Ref. Wu et al. (1995) contains more details on source number estimation). The element spacing is $d = \lambda/2$, where λ is the signal wavelength. We denote the DOA of the kth source as θ_k.

The received vector of sensors can be expressed as a linear system of equation, i.e.

$$\mathbf{y} = \mathbf{A}(\theta)\,\mathbf{s} + \mathbf{w}, \tag{1}$$

where $\mathbf{y} = [y_1, y_2, \ldots, y_M]^T$ is an $M \times 1$ received signal vector, $\mathbf{w}$ is an unknown noise vector, and $\mathbf{s} = [s_1, s_2, \ldots, s_K]^T$ is a $K \times 1$ signal vector. The quantity

$$\mathbf{A}(\theta) = \begin{bmatrix} \mathbf{a}(\theta_1)\ \mathbf{a}(\theta_2)\ \ldots\ \mathbf{a}(\theta_K) \end{bmatrix} \tag{2}$$

is called a steering matrix, where each column $\mathbf{a}(\theta_k)$ is a length-M vector with elements $e^{j\pi(m-1)\sin\theta_k}$, where $m = 1, 2, \ldots M$. Our source localization problem is to estimate the DOAs $\theta = \{\theta_k\}$ of sources given the single measurement $\mathbf{y}$. This is cast as an inverse problem. Thus, mathematically, it bears resemblance to problems such as superresolution image reconstruction (Chan et al. 2007), blind deconvolution (Xu and Lam 2009), or image synthesis (Chan et al. 2008).

2.2 General source localization methods based on a sparse representation

To solve Eq. (1) with a sparse representation, we can generalize the steering matrix $\mathbf{A}(\theta)$ to an overcomplete dictionary $\mathbf{D}$ in terms of all possible source locations $\left\{ \hat{\theta}_1, \ldots, \hat{\theta}_N \right\}$, such that

$$\mathbf{D} = \begin{bmatrix} \mathbf{a}(\hat{\theta}_1)\ \mathbf{a}(\hat{\theta}_2)\ \ldots\ \mathbf{a}(\hat{\theta}_N) \end{bmatrix}. \tag{3}$$

where N is the grid number, and that both $N \gg K$ and $N \gg M$. Correspondingly, the source vector $\mathbf{s}$ can be extended to an $N \times 1$ vector $\mathbf{h}$, where the nth element h_n is nonzero and equal to s_k if source k comes from $\hat{\theta}_n$, and zero otherwise.

For a single measurement vector (SMV), i.e., a single snapshot, Eq. (1) using the overcomplete dictionary $\mathbf{D}$ becomes

$$\mathbf{y} = \mathbf{D}\mathbf{h} + \mathbf{w}. \tag{4}$$

For this case, $\mathbf{h}$ is sparse, and this property can be used to improve the DOAs estimation. To use this as a constraint, we use the ℓ_0 norm to arrive at the following optimization, where we seek to

$$\begin{aligned} &\text{minimize} && \|\mathbf{h}\|_0 \\ &\text{subject to} && \|\mathbf{y} - \mathbf{D}\mathbf{h}\|_2^2 \leq \varepsilon, \end{aligned} \tag{5}$$

where $\|\mathbf{h}\|_0$ counts the number of nonzero entries in $|\mathbf{h}|$, and ε is the maximum acceptable error. However, finding a global minimum to the ℓ_0 norm minimization requires a combinatorial search that is computationally unattractive. Instead, we convert this problem into an ℓ_1 norm minimization as follows:

$$\begin{aligned} &\text{minimize} && \|\mathbf{h}\|_1 \\ &\text{subject to} && \|\mathbf{y} - \mathbf{D}\mathbf{h}\|_2^2 \leq \varepsilon, \end{aligned} \tag{6}$$

where the ℓ_1 norm is computed as $\|\mathbf{h}\|_1 = \sum_{n=1}^{N} |h_n|$.

The formulation in Eq. (6) can effectively handle the combinatorial problem in Eq. (5) under rather general conditions (Tropp 2004; Donoho 1995; Li et al. 2006).

With Lagrange multipliers we can write the solution to Equation (6) as

$$\hat{\mathbf{h}} = \arg\min_{\mathbf{h}} \|\mathbf{y} - \mathbf{D}\mathbf{h}\|_2^2 + \lambda \|\mathbf{h}\|_1. \tag{7}$$

This is a quadratic problem whose unique global minimum can be obtained using standard robust routines for quadratic programming (Lam 2007; Zhang and Lam 2009). Furthermore, it is known that for a normalized $\mathbf{D}$, when the regularization parameter λ is chosen as $\sigma \sqrt{2 \log N}$ with σ denoting the noise level, the optimal sparse solution can be approximately obtained (Fuchs 2001; Chen et al. 2001).

For multiple measurement vectors (MMV), let L be the measurement number. The vectors $\{\mathbf{y}_1, \ldots, \mathbf{y}_L\}$ are then the observed signals. Using the generic model in Eq. (1), we have

$$\mathbf{Y} = \mathbf{A}(\theta) \mathbf{S} + \mathbf{W}, \tag{8}$$

in which $\mathbf{Y} = [\mathbf{y_1}\ \mathbf{y_2} \ldots \mathbf{y_L}]$, $\mathbf{S} = [\mathbf{s_1}\ \mathbf{s_2} \ldots \mathbf{s_L}]$, and $\mathbf{W} = [\mathbf{w_1}\ \mathbf{w_2} \ldots \mathbf{w_L}]$. As with the derivation above, when we have a sparse representation framework using an overcomplete dictionary, we can encapsulate the signal formation as

$$\mathbf{Y} = \mathbf{D}\mathbf{H} + \mathbf{W}, \tag{9}$$

where $\mathbf{H} = [\mathbf{h_1}\ \mathbf{h_2} \ldots \mathbf{h_L}]$. The inverse problem solution is then

$$\hat{\mathbf{H}} = \arg \min_{\mathbf{H}} \|\mathbf{Y} - \mathbf{D}\mathbf{H}\|_{\mathrm{F}}^2 + \lambda \left\| \sum_{j=1}^{L} |\mathbf{h}_j| \right\|_1, \tag{10}$$

where $\|\cdot\|_{\mathrm{F}}$ denotes the Frobenius norm. The quantity $\sum_{j=1}^{L} |\mathbf{h}_j|$ will be a sparse vector after the optimization. The indices of nonzero rows of $\hat{\mathbf{H}}$ give the DOA estimates.

In the above methods, either SMV or MMV, the amplitude information of $\hat{\mathbf{h}}$ or $\hat{\mathbf{H}}$ is used to determine which entries are nonzero. We call these amplitude-based methods, and denote the estimated DOAs as $\hat{\theta}^{\mathrm{amp}}$.

2.3 Source localization using phase

Let $\mathbf{I}_{M-1}$ be an identity matrix of size $(M-1) \times (M-1)$, and $\mathbf{0}$ is an all-zero vector of length $(M-1)$. We define two permutation matrices, $\mathbf{J}_1$ and $\mathbf{J}_2$, where $\mathbf{J}_1 = [\mathbf{I}_{M-1}\ \mathbf{0}]$ and $\mathbf{J}_2 = [\mathbf{0}\ \mathbf{I}_{M-1}]$. By premultiplication of these permutation matrices, we can obtain two different parts of Eq. (4) where

$$\mathbf{y}_1 = \mathbf{J}_1 \mathbf{y} = \mathbf{J}_1 \mathbf{D}\mathbf{h} + \mathbf{J}_1 \mathbf{w} = \mathbf{D}_1 \mathbf{h} + \mathbf{w}_1 \tag{11}$$

$$\mathbf{y}_2 = \mathbf{J}_2 \mathbf{y} = \mathbf{J}_2 \mathbf{D}\mathbf{h} + \mathbf{J}_2 \mathbf{w} = \mathbf{D}_2 \mathbf{h} + \mathbf{w}_2, \tag{12}$$

where $\mathbf{y}_1 = [y_1, y_2, \ldots, y_{M-1}]^T$ and $\mathbf{y}_2 = [y_2, y_3, \ldots, y_M]^T$. The vector $\mathbf{w}$ is split into $\mathbf{w}_1$ and $\mathbf{w}_2$ in a similar fashion. In other words, $\mathbf{y}_1$ and $\mathbf{y}_2$ are the receiving vectors of two subarrays. Furthermore, $\mathbf{D_1} = \mathbf{J}_1 \mathbf{D}$ equals to $\mathbf{D}$ with the last row removed, and $\mathbf{D}_2 = \mathbf{J}_2 \mathbf{D}$ equals to $\mathbf{D}$ with the first row removed. Given the special structure in $\mathbf{D}$, we can relate the two quantities with a diagonal matrix ϕ as

$$\mathbf{D}_2 = \mathbf{D}_1 \phi, \quad \text{where} \quad \phi = \begin{bmatrix} e^{j\pi \sin \hat{\theta}_1} & & \\ & \ddots & \\ & & e^{j\pi \sin \hat{\theta}_N} \end{bmatrix}. \tag{13}$$

We can then combine Eqs. (11) and (12) as

$$\mathbf{Y} = [\mathbf{y}_1\ \mathbf{y}_2] = \mathbf{D}_1 [\mathbf{h}\ \phi\mathbf{h}] + [\mathbf{w}_1\ \mathbf{w}_2] = \mathbf{D}_1 \mathbf{H} + \mathbf{W}, \tag{14}$$

where $\mathbf{H} = [\mathbf{h} \ \phi\mathbf{h}] = [\mathbf{h}_1 \ \mathbf{h}_2]$. Compared with Eq. (9), it is obvious that the above is a special case of MMV, and the solution is described in Sect. 2.2. The estimation $\hat{\mathbf{H}}$ has a sparse structure. Consider an example of a two-source case, we have

$$\mathbf{h}_1 = [\ldots, h_{1i}, \ldots, h_{1j}, \ldots]^T \quad \text{and} \quad \mathbf{h}_2 = [\ldots, h_{2i}, \ldots, h_{2j}, \ldots]^T. \quad (15)$$

The nonzero entries in the same row of sparse solutions are related by

$$h_{1i} = e^{j\pi \sin \theta_i} h_{2i} \quad \text{where} \quad i = 1, \ldots, N. \quad (16)$$

Furthermore, the DOA estimate is given by

$$\hat{\theta}_i = \sin^{-1}\left(\frac{\text{angle}(\hat{h}_{2i}/\hat{h}_{1i})}{\pi}\right), \quad (17)$$

where angle($\cdot$) denotes phase operator, i.e., it returns the phase angle of a complex number, in radians. We denote the DOA estimation via the phase of the sparse solution $\hat{\theta}_i$ as $\hat{\theta}^{\text{pha}}$ for comparison.

2.4 A resampling technique to estimate DOA

Both $\hat{\theta}^{\text{amp}}$ and $\hat{\theta}^{\text{pha}}$ provide information for the DOA estimation. It is possible to give a better DOA estimation based on the two estimators without a refining grid strategy, using a computational technique called bootstrapping (Dasgupta and Michalewicz 1997; Zoubir and Iskander 2007).

Using the sparse solution $\hat{\mathbf{H}}$, we can reconstruct the receiving data $\hat{\mathbf{Y}}$ as

$$\hat{\mathbf{Y}} = \mathbf{D}_1 \hat{\mathbf{H}}. \quad (18)$$

Correspondingly, the noise matrix estimation can be given by

$$\hat{\mathbf{W}} = \mathbf{Y} - \hat{\mathbf{Y}} = \mathbf{Y} - \mathbf{D}_1 \hat{\mathbf{H}}. \quad (19)$$

We can assume that the residuals $\hat{\mathbf{W}}$ is approximately Gaussian and independent identically distributed (i.i.d.), and therefore can sample the residuals $\hat{\mathbf{W}}$ using the bootstrap method by drawing at random with replacement from $\hat{\mathbf{W}}$. We denote them as $\mathbf{W}^* = \{\mathbf{W}_1^*, \mathbf{W}_2^*, \ldots, \mathbf{W}_B^*\}$, where B is the number of bootstrap samples. The resampling of the receiving data of sensors $\mathbf{Y}^* = \{\mathbf{Y}_1^*, \mathbf{Y}_2^*, \ldots, \mathbf{Y}_B^*\}$ can then be rewritten as

$$\mathbf{Y}_b^* = \mathbf{D}_1 \hat{\mathbf{H}} + \mathbf{W}_b^*, \quad (20)$$

where $b = 1, \ldots, B$. For a large B, we can give the DOA estimation using both the amplitude-based and the phase-based methods, which are denoted as $\hat{\theta}_b^{\text{amp}}$ and $\hat{\theta}_b^{\text{pha}}$, respectively. A reasonable mean and variance of DOA estimation with the two methods are

Table 1 The DOAs estimation using bootstrap resampling

Step 1	Use amplitude and phase of sparse solution to compute $\hat{\theta}^{\text{amp}}$ and $\hat{\theta}^{\text{pha}}$
Step 2	Based on the sparse solution, reconstruct $\hat{\mathbf{Y}}$ using Eq. (18) and $\hat{\mathbf{W}}$ using Eq. (19)
Step 3	Resample $\hat{\mathbf{W}}$ using bootstrap method as well as $\mathbf{Y}_b^*$ using Eq. (20)
Step 4	Compute the mean and variance of DOAs estimation from Eqs. (21, 22, 23 and 24) using bootstrap resampling
Step 5	The ultimate DOAs estimation can be obtained from Eq. (25)

$$\bar{\theta}_B^{\text{amp}} = \frac{1}{B} \sum_{b=1}^{B} \hat{\theta}_b^{\text{amp}} \tag{21}$$

$$\bar{\theta}_B^{\text{pha}} = \frac{1}{B} \sum_{b=1}^{B} \hat{\theta}_b^{\text{pha}} \tag{22}$$

$$\text{var}\left(\hat{\theta}_B^{\text{amp}}\right) = \frac{1}{B} \sum_{b=1}^{B} \left(\hat{\theta}_b^{\text{amp}} - \bar{\theta}_B^{\text{amp}}\right)^2 \tag{23}$$

$$\text{var}\left(\hat{\theta}_B^{\text{pha}}\right) = \frac{1}{B} \sum_{b=1}^{B} \left(\hat{\theta}_b^{\text{pha}} - \bar{\theta}_B^{\text{pha}}\right)^2. \tag{24}$$

From a statistical point of view, a smaller variance leads to a more precise DOA estimation. The latter can be given by

$$\hat{\theta}^{\text{x}} = \min_{\text{x} \in \{\text{amp}, \text{pha}\}} \text{var}\left(\hat{\theta}_B^{\text{x}}\right). \tag{25}$$

In order to evaluate the performance of bootstrap sampling, we define the success probability γ as

$$\gamma = \frac{|\hat{\theta}^{\text{x}} - \theta|}{\min\left(|\hat{\theta}^{\text{pha}} - \theta|, |\hat{\theta}^{\text{amp}} - \theta|\right)}. \tag{26}$$

The closer γ is to one, the better the performance of our method is.

The overall source localization approach using the sparse solution is summarized in Table 1.

3 Discussions

We want to highlight three points regarding the above algorithm: First, although our discussion above considers only two subarrays, the technique can be easily generalized to more subarrays, which contain more phase information. On the other hand, too many subarrays will degenerate the performance of DOA estimation (Wang et al. 2006), and therefore a reasonable number of subarrays should be less than $M - K$ but more than two. Second, for brevity we also only consider the ULA case. The method can extend to other manifolds if the rotational invariance property is satisfied, such as for uniform circular array (UCA), uniform plane array, etc. Third, although the main idea of our method comes from an ESPRIT-type method (Roy et al. 1986), as a subspace method, the latter cannot give a satisfactory DOA

Table 2 RMSE of amplitude- and phase-based methods under different grid distances

Grid distance (degrees)		5	2.5	1	0.5	0.1	0.01	0.001
SNR (20 dB) $\theta = -11.7°$	$\hat{\theta}_{\text{RMSE}}^{\text{amp}}$	0.7506	0.7068	0.3386	0.2356	0.1518	0.1322	0.1176
	$\hat{\theta}_{\text{RMSE}}^{\text{pha}}$	0.3006	0.1982	0.1786	0.1697	0.1438	0.1660	0.1635

estimation when the number of measurement vectors is too few. Additionally, the amplitude-based and phase-based methods will give different results depending on whether the true DOA is on the grid or not. In either case, we will show that the resampling technique can give the optimal estimates.

4 Simulation results

In this section, we present simulation results to demonstrate the efficacy of the proposed method. The inverse problem of Eq. (14), cast as a convex optimization problem, is solved by SPGL1 (Berg and Friedlander 2007). An additive white Gaussian noise is considered and the signal-to-noise ratio (SNR) is defined as $= 10 \log_{10} \left(\sigma_s^2 / \sigma^2 \right)$, where σ_s^2 is the signal power. We can fix $\sigma_s^2 = 1$ in our simulation and the values of σ can be computed from different SNRs.

4.1 The performance of amplitude- and phase-based methods under different grid distances

We compare the performance of amplitude-based and phase-based methods under different grid distances. First, in our simulation we fix the sensor element $M = 8$. The spatial frequency is defined as $f = \frac{1}{2} \sin \theta$, where θ is measured in degrees. We have $-0.5 \leq f \leq 0.5$. Seven different grid distances between adjacent grids of 5, 2.5, 1, 0.5, 0.25, 0.05 and 0.001 degrees are considered, with their corresponding grid distance calculated using the spatial frequency formula above. The possible DOAs are from $-90°$ to $90°$. In order to show the relationship between the grid number and source localization performance, we consider SNR $= 20$dB and $\theta = -11.7°$ case (chosen at random). A total of $P = 200$ Monte Carlo simulations are conducted. We define the root-mean-square error (RMSE) of the two methods as

$$\theta_{\text{RMSE}} = \sqrt{\frac{1}{P} \sum_{p=1}^{P} \left(\theta - \hat{\theta}_p \right)^2}, \tag{27}$$

where θ is the true DOA, and $\hat{\theta}_p$ comes from the pth DOA estimates of $\hat{\theta}_p^{\text{pha}}$ and $\hat{\theta}_p^{\text{amp}}$. Table 2 shows the RMSE of $\hat{\theta}^{\text{amp}}$ and $\hat{\theta}^{\text{pha}}$ under different grid distances. It shows that for a large grid distance the RMSE of phase-based method is smaller than amplitude-based method, while for a small grid distance, the performance is reversed. Hence, we can combine the two methods to give a more precise DOA estimate based on bootstrap resampling.

4.2 The localization error for two different cases

Suppose we have two different sources at 60° and 60.5°, respectively. Since the possible source DOAs are confined to be between $-90°$ and $90°$, and the distance between adjacent grids is 1°, the resulting grid number is $N = 181$. The DOA estimation errors with 200
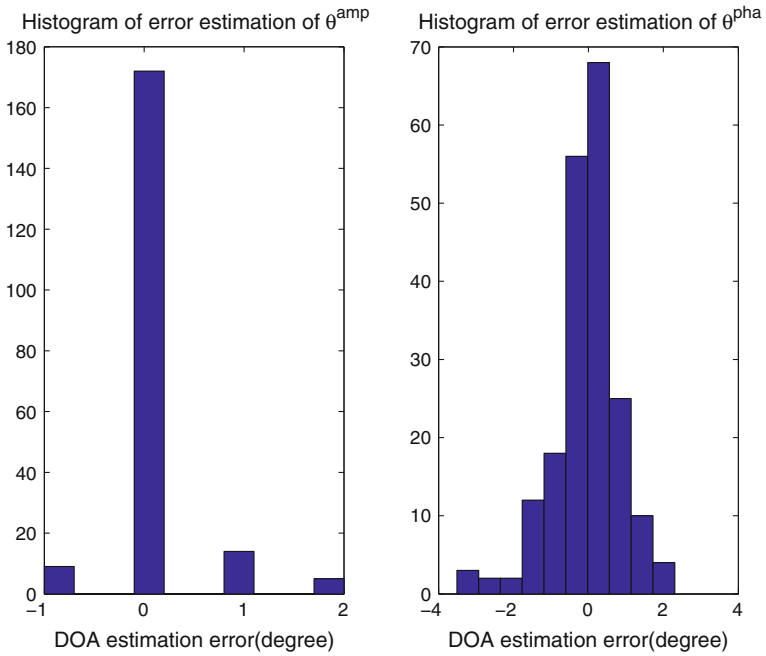
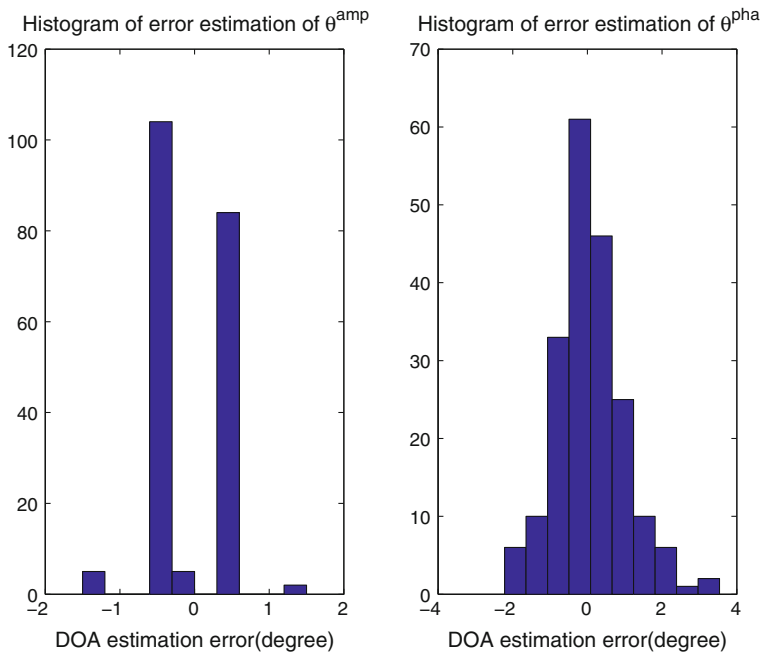**Fig. 2** The histogram of DOAs estimation errors for $M = 10$, SNR $= 15$ dB, and $\theta = 60°$

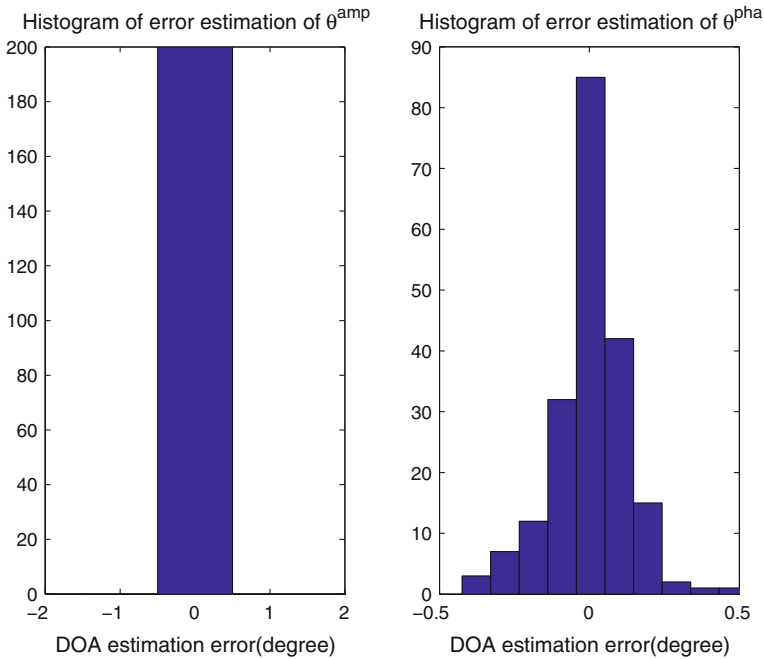**Fig. 3** The histogram of DOAs estimation errors for $M = 10$, SNR $= 15$dB, $\theta = 60.5°$

Fig. 4 The histogram of DOAs estimation errors for $M = 16$, SNR $= 30$ dB, $\theta = 60°$

independent trials are shown in Figs. 2 and 3 where the sensor number is 10 and the SNR is 15 dB. For the case that the sensor number is 16 and SNR $= 30$ dB, the DOA estimation errors are depicted in the histograms shown in Figs. 4 and 5.

From the four figures, we can see that the DOA estimations from $\hat{\theta}^{\text{pha}}$ and $\hat{\theta}^{\text{amp}}$ are more precise when the SNR and M are both higher, which certainly agrees with our expectation. As discussed in Sect. 3, the coherence of the overcomplete dictionary can be improved by increasing the sensor number, grid distance and SNR. Because the grid distance in our example is fixed to $1°$, the remaining factors will influence the performance of source localization, as shown in Figs. 2–5.

Next we consider the grid influence on the performance of source localization. Firstly, if the true DOA is not on the grid where we generate the overcomplete dictionary, the fixed bias of DOA estimation via the amplitude-based method $\hat{\theta}^{\text{amp}}$ must exist regardless whether M and SNR are lower or higher, while the phase-based method $\hat{\theta}^{\text{pha}}$ can deal with this case efficiently. On the contrary, if the DOA to be estimated is exactly on the grid, the amplitude-based method is expected to give more precise source localization results, as seen from the two figures. In other words, the amplitude-based method is useful only when the true DOA is exactly on the grid, which is not always possible.

4.3 Comparison with other methods and Cramer-Rao Bound

Assume there are 8 sensors. All possible DOA locations are from $-90°$ to $90°$ and the distance between adjacent grids is $0.1°$, so the grid number is $N = 1801$. The DOA of one source is randomly generated within $[-30°, 30°]$. The SNR varies from 0 to 40 dB with a step size of
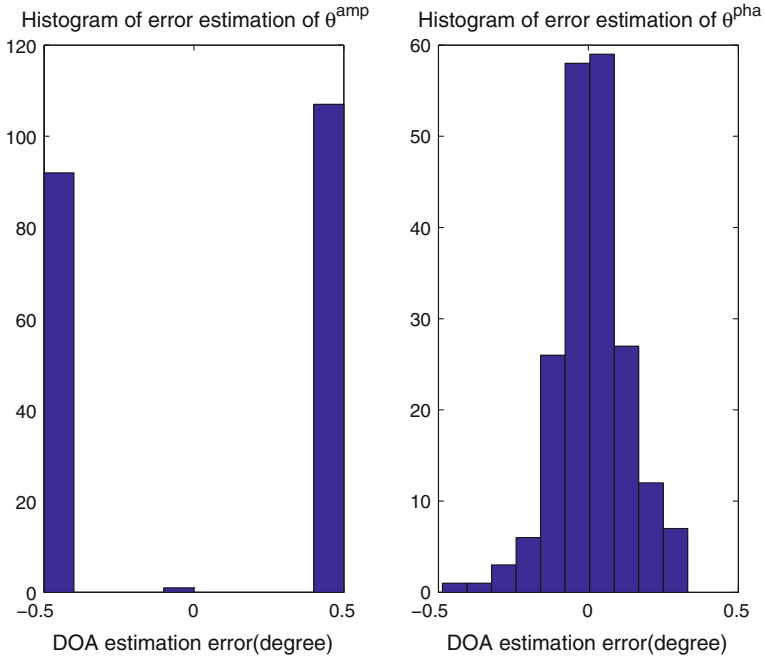
Fig. 5 The histogram of DOAs estimation errors for $M = 16$, SNR $= 30$dB, $\theta = 60.5°$
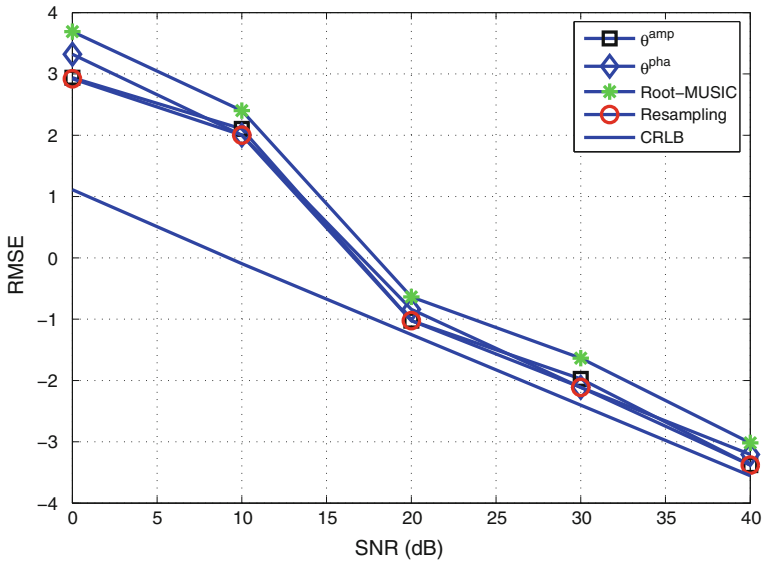

Fig. 6 The RMSE of DOAs estimation versus SNR for different methods

5 dB. For easy comparison, the DOA estimation using conventional Root-MUSIC (see the work of Weiss and Friedlander (1993) for more details) method is also given. For the three different methods, the RMSE of DOA estimates versus SNR, together with the Cramer-Rao

Table 3 The success probability of our method with different numbers of bootstrap samples

B	10	30	50	100	200
γ	0.614	0.863	0.912	0.975	0.999

bound (Gershman et al. 2002), are plotted in Fig. 6. Note that this is a logarithmic plot. It shows that Root-MUSIC, as a conventional subspace method, has a worse performance compared with the sparsity-based methods (amplitude-based and phase-based) because we use only a single measurement vector to estimate the DOA of sources. For the latter, the proposed bootstrap resampling technique can determine the optimal DOA estimation from the amplitude-based and phase-based estimation regardless of whether the DOA is on the grid or not.

4.4 Selection of the number of bootstrap samples

The sampling number is a key problem affecting the performance of our method. In general, more bootstrap samples imply better performance. For example, let there be 12 sensors and that the true DOA comes from 30°. The SNR is fixed at 30 dB. For simplicity, the different values of B is taken from 10 to 200 with different separation distances. Table 3 lists the effects of the number of bootstrap samples. A small B (such as $B = 10$) gives a poor performance. However, when we use 200 times independent sample, the success probability is almost one, achieving highly precise estimation results.

5 Conclusion

In this paper, we propose a source localization approach under the sparse representation framework. The bootstrap resampling technique is derived to determine the optimal DOA estimation. By combining the amplitude and phase information of sparse solution, the proposed method can improve the source localization precision efficiently.

References

Berg, E. V., Friedlander, M. P. (2007). SPGL1: A solver for large-scale sparse reconstruction, June, http://www.cs.ubc.ca/labs/scl/spgl1.

Chan, W. S., Lam, E. Y., Ng, M. K., & Mak, G. Y. (2007). Super-resolution reconstruction in a computational compound-eye imaging system. *Multidimensional Systems and Signal Processing, 18*(2), 83–101.

Chan, S. H., Wong, A. K., & Lam, E. Y. (2008). Initialization for robust inverse synthesis of phase-shifting masks in optical projection lithography. *Optics Express, 16*(19), 14746–14760.

Chen, J., & Huo, X. (2006). Theoretical results on sparse representations of multiple-measurement vectors. *IEEE Transactions on Signal Processing, 54*(12), 4634–4643.

Chen, S. S., Donoho, D. L., & Saunders, M. A. (2001). Atomic decomposition by basis pursuit. *SIAM Review, 43*, 129–159.

Chow, K.-Y., Lui, K.-S., & Lam, E. Y. (2007). Efficient on-demand image transmission in visual sensor networks. *EURASIP Journal on Advances in Signal Processing, 2007*, 95076(11p).

Chow, K.-Y., Lui, K.-S., & Lam, E. Y. (2009). Wireless sensor networks scheduling for full angle coverage. *Multidimensional Systems and Signal Processing, 20*(2), 101–119.

Cotter, S. F., Kreutz-Delgado, K., & Rao, B. D. (2002). Efficient backward elimination algorithm for sparse signal representation using overcomplete dictionaries. *IEEE Signal Processing Letters, 9*(5), 145–147.

Dasgupta, D., & Michalewicz, Z. (1997). *Evolutionary algorithms in engineering applications*. Berlin: Springer.

Donoho, D. (1995). De-noising by soft-thresholding. *IEEE Transactions on Information Theory, 41*(3), 613–627.

Fuchs J. J. (1998). *Detection and estimation of superimposed signals*. ser. Proc. ICASSP (vol. III, pp. 1649–1652), Seattle, May.

Fuchs, J. J. (2001). On the application of the global matched filter to DOA estimation with uniform circular arrays. *IEEE Transactions on Signal Processing, 49*(4), 702–709.

Gershman, A., Stoica, P., Pesavento, M., & Larsson, E. (2002). Stochastic Cramer-Rao bound for direction estimation in unknownnoise fields. *IEE Proceedings-Radar, Sonar and Navigation, 149*(1), 2–8.

Gorodnitsky, I. F., & Rao, B. D. (1997). Sparse signal reconstructions from limited data using FOCUSS: A re-weighted minimum norm algorithm. *IEEE Transactions on Signal Processing, 45*(3), 600–616.

Lam, E. Y. (2007). Blind bi-level image restoration with iterated quadratic programming. *IEEE Transactions on Circuits and Systems II, 549*(1), 52–56.

Li, Y., Amari, S., Cichocki, A., & Guan, C. (2006). Probability estimation for recoverability analysis of blind source separation based on sparse representation. *IEEE Transactions on Information Theory, 52*(7), 3139–3152.

Maria, S., & Fuchs, J. J. (2006) *Application of the global matched filter to STAP data: An efficient algorithmic approach*. ser. Proc. ICASSP (Vol. 4, pp. 14–19).

Malioutov, D., Cetin, M., & Willsky, A. S. (2005). A sparse signal reconstruction perspective for source localization with sensor arrays. *IEEE Transactions on Signal Processing, 53*(8), 3010–3022.

Roy, R., Paulraj, A., & Kailath, T. (1986). ESPRIT—A subspace rotation approach to estimation of parameters of cisoids in noise. *IEEE Transactions on Acoustics, Speech and Signal Processing, 34*(5), 1340–1342.

Schmidt, R. O. (1986). Multiple emitter location and signal parameter estimation. *IEEE Transactions on Antennas and Propagation, 34*(3), 276–280.

Tropp, J. A. (2004). Topics in sparse approximation. Ph.D. dissertation, The Unverisity of Texas at Austin, TEXAS.

Wang, N., Agathoklis, P., & Antoniou, A. (2006). A new DOA estimation technique based on subarray beamforming. *IEEE Transaction on Signal Processing, 54*(9), 3279–3290.

Weiss, A. J., & Friedlander, B. (1993). Direction finding for diversely polarized signals using polynomial rooting. *IEEE Transaction on Signal Processing, 41*(5), 1893–1905.

Wu, H. T., Yang, J. F., & Chen, F. K. (1995). Source number estimators using transformed gerschgorin radii. *IEEE Transactions on Signal Processing, 43*(6), 1325–1333.

Xu, Z., & Lam, E. Y. (2009). Maximum a posteriori blind image deconvolution with Huber-Markov random-field regularization. *Optics Letters, 34*(9), 1453–1455.

Zhang, X., & Lam, E. Y. (2009). Superresolution reconstruction using nonlinear gradient-based regularization. *Multidimensional Systems and Signal Processing, 20*(4), 375–384.

Zoubir, A. M., & Iskander, D. R. (2007). Bootstrap methods and applications. *IEEE Signal Processing Magazine, 24*(4), 10–19.